Structure of colloidal crystals in sedimenting mixed dispersions of latex and silica particles

Tadatomi Shinohara,* Toshiaki Kurokawa, Tsuyoshi Yoshiyama,† Takamasa Itoh,‡ and Ikuo S. Sogami§
Department of Physics, Kyoto Sangyo University, Kita-ku, Kyoto 603-8555, Japan

Norio Ise‖
Kyoto University, Kyoto 606-8501, Japan
(Received 19 June 2004; published 28 December 2004)

We report bcc-fcc transitions of colloidal crystals in mixed aqueous dispersions of polystyrene-based latex particles (diameter: $D=55.8$ nm) and silica particles (diameter: $D=170$ nm). In the single systems, the silica particles formed bcc crystals and the latex particles did not crystallize. In the binary mixtures of these particles, colloidal crystals with fcc structures were found by the analysis of Kikuchi-Kossel diffraction images. Especially, the samples at low latex fractions started out as bcc structures, and then changed to fcc structures. Due to gravitational sedimentation, the lattice constant increased as the height from the bottom of the dispersion became larger. Furthermore, the lattice constant became smaller at a given silica fraction as the latex fraction increased.

DOI: 10.1103/PhysRevE.70.062401 PACS number(s): 82.70.Dd, 42.25.Fx, 61.66.Dk

I. INTRODUCTION

In 1928, Kikuchi [1] observed a characteristic diffraction image from a mica using electron beams. In 1934, Kossel [2] discovered a similar diffraction image from a copper crystal using fluorescent x rays, and established the interpretation of the observed images. According to the principle of Fourier transformation, scattering from a crystal plane is observed as a point. On the other hand, Kikuchi-Kossel (KK) diffraction patterns from a crystal plane consist of curves. Accordingly, the KK diffraction method can provide structural information on colloidal crystals with high precision [3–5]. Using the KK technique, the crystallization in colloidal dispersions of highly charged latex particles was found to proceed via multiphases [6] to form a colloidal crystal with a face-centered-cubic (fcc) structure and/or body-centered-cubic (bcc) structure in dilute dispersions [7]. Subsequently, we investigated colloidal crystals of silica particles with a density of 2.2 g/cm^3 in water and noticed small but distinct gravitational sedimentation effects [8,9] of the particles.

For binary systems consisting of two latex particles with different sizes, alloy structures were reported by Hachisu and Yoshimura [10]. Although it was highly interesting, the result was obtained by metallurgical microscopic observation, which provides accurate but only local information. Thus, the possibility that the information obtained may not be valid throughout the whole dispersion cannot be completely ruled out. Recently, Okazaki and Yoshiyama [11] observed stable colloidal crystals with a stacking structure with multivariant periodicity for two mixtures of two latex particles [average diameter D:(77 nm+156 nm) and (77 nm +217 nm)] by means of the KK diffraction method. Experimental research into phase diagrams for mixed systems has also been performed by many authors [12–15].

In this Brief Report, we report bcc-fcc transitions of colloidal crystals in binary systems consisting of latex and silica particles. The samples used in the present work were latex particles of $D=55.8$ nm and silica colloids of $D=170$ nm. We mixed the two dispersions in various ratios. When the fraction of the latex particles in the mixed solution was small, colloidal crystals with fcc structure were found by analysis of the KK diffraction images. In the single-component dispersions prior to the mixing, the small latex particles did not crystallize, whereas the silica particles formed a bcc structure, as shown in Refs. [8,9]. We note that by carrying out the KK diffraction measurement at various heights of the dispersions, it was possible to obtain accurately not only local but also overall structural information.

II. EXPERIMENT

The colloidal particles used were colloidal silica Seahoster KE-E20 produced by Nippon Shokubai Co., Ltd. (Osaka, Japan) and polystyrene-based latex N558 produced by Sekisui Chemical Co. (Osaka, Japan), which have D of 170 and 55.8 nm, respectively. The particle size distributions were about $\sigma/D\approx 5\%$ for the KE-E20, as shown in Ref. [16], and $\sigma/D=8.78\%$ for the N558, where σ denotes the standard deviation of the particle diameter distribution. After purification with Milli-Q water and deionization by ion-exchange resin particles, the effective surface charge densities of the colloidal particles were determined to be $0.15\mu C/cm^2$ for the silica particles and $0.70\mu C/cm^2$ for the latex particles by the method described earlier [16–18]. To exclude the influence of any ionic strength distribution (caused by relatively slow deionization processes by the ion-exchange resins) among several samples, to minimize impurity ions from outside, and to avoid evaporation of the liquids inside, all the samples were introduced into hermetically

*Electronic address: sinohara@cc.kyoto-su.ac.jp
†Electronic address: yosiyama@cc.kyoto-su.ac.jp
‡Electronic address: physik@cc.kyoto-su.ac.jp
§Electronic address: sogami@cc.kyoto-su.ac.jp
‖Electronic address: norioise@sea.plala.or.jp

TABLE I. Binary mixtures of latex and silica particles.

Sample name	A	B	C	D	E	F
Volume (latex [ml] ; silica [ml])[a]	0; 4.5	0.03; 4.5	0.06; 4.5	0.09; 4.5	0.12; 4.5	4.5; 0
Number ratio (latex:silica)	0:1	1:4.02	1:2.01	1:1.34	1:1.00	1:0
Volume fraction [b] (ϕ_{la}; ϕ_{si})	0; 0.0225	0.00020; 0.0224	0.00039; 0.0222	0.00058; 0.0221	0.00077; 0.0219	0.0297; 0
Lattice symmetry	bcc	bcc-fcc	fcc	fcc	fcc	No crystal

[a]The volume fractions of the dispersion are $\phi_{la}=0.0297$ and $\phi_{si}=0.0225$.
[b]For the whole dispersion.

sealed quartz cuvettes (height 45 mm; width 10 mm; inner thickness 1 mm) with an air-tight lid. Ion-exchange resins were not added. The dispersions began to show iridescence due to the formation of microcrystals after their introduction into the cuvettes, but the speeds of crystal growth varied from sample to sample. The cuvettes were kept standing vertically, and the temperature was held at room temperature.

The KK diffraction experiments were conducted in the same manner as described earlier [3,5,19]. On the supposition that the cuvette's quartz plate is infinitely thin, we considered refraction at the boundary between the colloidal crystal surface and air. To correct for the refractive effect by using Snell's law, we adopted the formula for the refractive index of colloidal dispersions $n(\phi_{si}, \phi_{la})$ proposed by Hiltner and Krieger [20]

$$n(\phi_{si}, \phi_{la}) = n_{wa}(1 - \phi_{si} - \phi_{la}) + n_{si}\phi_{si} + n_{la}\phi_{la}, \qquad (1)$$

where n_{wa}, n_{si}, and n_{la} are the refractive indices of water, silica particle, and latex particle ($n_{wa}=1.33, n_{si}=1.47$ [21,22], and $n_{la}=1.60$), respectively. Likewise, ϕ_{si} and ϕ_{la} are the volume fractions of the silica and latex particles in the dispersions, respectively. We used an Ar laser of wavelength 488 nm.

III. RESULTS AND DISCUSSION

We made mixed dispersions with a single dispersion ($\phi_{si}=0.0225$) of the silica particles KE-E20 and one ($\phi_{la}=0.0297$) of the latex particles N558 at various ratios to prepare the six samples shown in Table I. In addition to the samples A–F, we also prepared very dilute dispersions ($\phi_{la}=0.0006$ and 0.0019) of the latex particles. No crystallization was observed in these dispersions. Samples A and B began to show iridescence due to microcrystals formed throughout the container within a few minutes after their introduction into the cuvettes. For samples C, D, and E, crystallization was noticed up to elevations of 27, 4, and 2 mm from the bottom of the cuvette in half a day, on the second day, and the seventh day, respectively. Sample B showed homogeneous nucleation and underwent gravitational settling. In samples C–E, settling preceded, and homogeneous nucleation took place subsequently. Figure 1 shows the pictures photographed on the 161st day after introduction of the dispersion for samples B (left) and F (right).

The KK diffraction images for samples A, B, and C were taken on the first day after introduction of the samples into the container. The colloidal crystals of sample A were found to have bcc structures (lattice constants: 613–631 nm) throughout the container (Fig. 2) and maintain bcc structures (see experiments 4–6 of Table II). In sample C, we observed fcc structures with lattice constants of 740–747 nm up to an elevation of 27 mm (experiments 20–22). It is hard to accept that the colloidal crystals of fcc structure in such a large region were formed only by the latex particles, although fcc structures were actually observed for other latex particles [5] at the concentration presently employed. In sample B, fcc and bcc structures were found to coexist. We repeated the experiments under the same condition and found the samples at low latex fractions started out as bcc and then changed to fcc. The regions of bcc structure of sample B decreased with the progress of time.

FIG. 1. (Color) Pictures of samples B (left) and F (right). The photograph was taken on the 161st day after the dispersion was introduced into the cuvette. Although sample B shows iridescence, the appearance of sample F indicates that no crystallization took place.

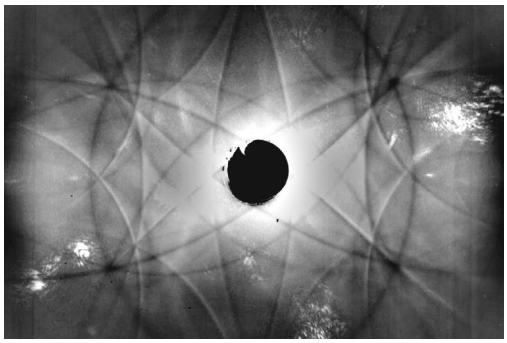

FIG. 2. Kikuchi-Kossel images of a colloidal crystal with a bcc structure. The picture was taken for sample A, a dispersion containing only KE-E20 silica particles with a volume fraction of 0.0225, at 31 mm from the bottom of the cuvette, on the first day after introduction of the dispersion into the container (experiment 2). The lattice constant is 625 nm.

TABLE II. Lattice constant.

Experiment	Days after introduction into cuvette	Height from the cuvette bottom (mm)	Lattice constant (nm)	Crystalline portion [a] (mm)	Crystal structure
		Sample A			
1	1	5	613	45	bcc
2	1	31	625	45	bcc
3	1	37	631	45	bcc
4	145	5	559	45	bcc
5	145	25	634	45	bcc
6	145	42	735	45	bcc
		Sample B			
7	1	16	767	45	fcc
8	1	16	605	45	bcc
9	1	21	766	45	fcc
10	1	39	608	45	bcc
11	7	31	785	32	fcc
12	7	32	787	32	fcc
13	15	31	793	31	fcc
14	47	10	712	35	fcc
15	47	15	734	35	fcc
16	47	21	754	35	fcc
17	47	25	774	35	fcc
18	47	30	790	35	fcc
19	47	35	818	35	fcc
		Sample C			
20	1	7	740	27	fcc
21	1	14	747	27	fcc
22	1	27	747	27	fcc
23	3	7	729	7	fcc
24	7	7	714	7	fcc
25	15	10	713	10	fcc
26	47	5	676	17	fcc
27	47	7	686	17	fcc
28	47	12	710	17	fcc
29	47	17	732	17	fcc
		Sample D			
30	3	3	688	4	fcc
31	3	4	690	4	fcc
32	7	5	678	5	fcc
33	15	6	674	6	fcc
34	47	4	658	13	fcc
35	47	8	671	13	fcc
36	47	13	688	13	fcc
		Sample E			
37	12	2	653	2	fcc
38	15	3	651	3	fcc
39	47	5	648	9	fcc
40	47	9	663	9	fcc

[a]The height of crystalline portion from the bottom of the cuvette.

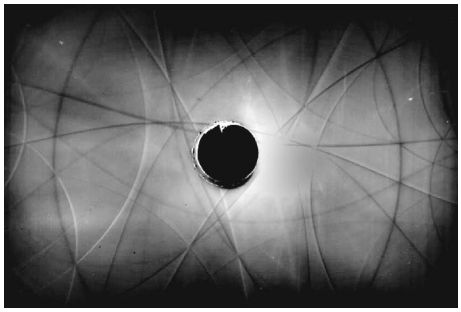

FIG. 3. Kikuchi-Kossel image of a colloidal crystal with an fcc structure. The photograph was taken from a colloidal crystal at an elevation of 32 mm from the bottom of the cuvette on the seventh day after the dispersion was introduced into the cuvette (experiment 12). The lattice constant is 787 nm. Sample B: KE-E20 silica particles at $\phi_{si}=0.0224$ and N558 latex particles at $\phi_{la}=0.00020$.

On the third day, the iridescent (crystalline) portions in samples B, C, and D were found in lower parts, at the elevations of 36, 7, and 4 mm from the bottom of the container, respectively. The fluid phase was noticed on top of these crystalline phases. Then, for the samples C and D, we observed fcc structures with lattice constants of 729 nm (experiment 23) and 690 nm (experiment 31), respectively, at the boundary between the crystalline phase and the fluid phase. Later, on the seventh day, the heights of the crystalline regions in samples B, C, D, and E were 32, 7, 5, and 2 mm, respectively, and the lattice constants in samples B, C, and D were 787 nm (experiment 12), 714 nm (experiment 24), and 678 nm (experiment 32) at the boundary between the crystalline and the fluid phases (sample B: see Fig. 3). We carried out the KK analysis for sample E on the 12th day and obtained a lattice constant of 653 nm (experiment 37) at an elevation of 2 mm. Although we observed colloidal crystals of fcc structure for samples B–E, the sizes and the lattice constants of the crystals were different. The results of these measurements are summarized in Table II.

Two tendencies are noteworthy in Table II. First, with the progress of time, the lattice constants increased in the upper part (at a height of 31 mm for sample B) from 785 to 790 nm (experiments 11, 13, and 18) and decreased in the lower part (at 7 mm for sample C) from 740 to 686 nm (experiments 20, 23, 24, and 27). For samples B–E on the 47th day, the lattice constants were larger with ascending elevation (experiments 14–19, 26–29, 34–36, and 39 and 40). These observations are due to a concentration gradient caused by gravitational sedimentation, as observed previously by Crandall and Williams [23] and ourselves [8]. Second, the lattice constants became smaller as the latex fraction increased at a given height (for example, experiments 14, 27, 35, and 40).

In the case where the whole dispersion is considered to be filled with a single crystal, the lattice constant a_0 of the colloidal crystal and the volume fraction ϕ are related by

$$a_0 = \sqrt[3]{\frac{16\pi}{3\phi}}R \quad \text{(for fcc)}, \qquad \sqrt[3]{\frac{8\pi}{3\phi}}R \quad \text{(for bcc)}, \quad (2)$$

where R is the radius of the colloidal particle. Since the volume fractions of each particle are as given in Table I, we

can obtain the lattice constants in the case where each component crystallizes independently of the other component. In sample B (experiments 7–10), fcc structure and bcc structure coexist (see Table II). Using Eq. (2), the lattice constants are obtained as 772 nm (silica) and 1221 nm (latex) for fcc, and 612 nm (silica) and 969 nm (latex) for bcc. The observed lattice constants were 766–767 nm (fcc) and 605–608 nm (bcc), being close to those expected for pure silica crystals. Therefore, it is thought that the small particles have been "buried" into the lattice structures which the large particle formed. However, the detailed mechanism is unsolved.

The alloy structure of the mixed system was interpreted in term of a packing model of a hard-sphere colloid [10,24]. Namely, the alloy structure is determined by the highest packing efficiency of a hard-sphere colloid. It is interesting to note that in the previous research the AB_5 structure, which has not been observed for actual atomic systems, has been found for the colloidal particle systems [10]. This may be due to a gravitational effect for the colloidal particles. It has been reported [25] that the fcc structure observed for silica particles of large size was due to the gravitational effect, and this may be connected with the result for the mixed systems shown here.

IV. CONCLUSIONS

We observed that binary dispersions of silica particles and latex particles formed an fcc structure, while silica alone formed a bcc structure and the latex particles did not crystallize. Due to gravitational sedimentation, the lattice constant increased as the height from the bottom of the dispersion became larger.

We also mixed other small latex particles (X-1:D = 77 nm, N-087:D = 87 nm) with the silica particle KE-E20, and observed fcc structures, in accordance with the present results.

ACKNOWLEDGMENTS

We thank Dr. Martin V. Smalley for his careful reading of the manuscript and suggestions. We wish to express our sincere thanks to Dr. Junpei Yamanaka, Faculty of Pharmaceutical Sciences, Nagoya City University, Japan, for advice. This study was partially funded by "Ground Research for Space Utilization" promoted by the Japan Aerospace Exploration Agency (JAXA) and the Japan Space Forum (JSF).

[1] S. Kikuchi, Jpn. J. Phys. **5**, 83 (1928).
[2] W. Kossel, V. Loeck, and H. Voges, Z. Phys. **94**, 139 (1935).
[3] T. Yoshiyama, I. Sogami, and N. Ise, Phys. Rev. Lett. **53**, 2153 (1984).
[4] T. Yoshiyama and I. S. Sogami, Phys. Rev. Lett. **56**, 1609 (1986).
[5] T. Yoshiyama and I. S. Sogami, in *Ordering and Phase Transitions in Charged Colloids*, edited by A. K. Arora and B. V. R. Tata (VCH, New York, 1996), pp. 41–68.
[6] I. S. Sogami and T. Yoshiyama, Phase Transitions **21**, 171 (1990).
[7] K. Ito, H. Nakamura, and N. Ise, J. Chem. Phys. **85**, 6136 (1986).
[8] T. Shinohara, T. Yoshiyama, I. S. Sogami, T. Konishi, and N. Ise, Langmuir **17**, 8010 (2001).
[9] T. Shinohara, H. Yamada, I. S. Sogami, N. Ise, and T. Yoshiyama, Langmuir **20**, 5141 (2004).
[10] S. Hachisu and S. Yoshimura, Nature (London) **283**, 188 (1980).
[11] H. Okazaki and T. Yoshiyama, in the Second Symposium on Advanced Photon Research, Kyoto, Japan, 2000 (unpublished).
[12] P. Bartlett, R. H. Ottewill, and P. N. Pusey, Phys. Rev. Lett. **68**, 3801 (1992); N. Hunt, R. Jardine, and P. Bartlett, Phys. Rev. E **62**, 900 (2000).
[13] A. Meller and J. Stavans, Phys. Rev. Lett. **68**, 3646 (1992).
[14] S. R. Williams and W. van Megen, Phys. Rev. E **64**, 041502 (2001).
[15] J. Liu and T. Palberg, Prog. Colloid Polym. Sci. **123**, 222 (2004).
[16] J. Yamanaka, N. Ise, H. Miyoshi, and T. Yamaguchi, Phys. Rev. E **51**, 1276 (1995).
[17] J. Yamanaka, H. Yoshida, T. Koga, N. Ise, and T. Hashimoto, Phys. Rev. Lett. **80**, 5806 (1998).
[18] H. Yoshida, J. Yamanaka, T. Koga, T. Koga, N. Ise, and T. Hashimoto, Langmuir **15**, 2684 (1999).
[19] T. Yoshiyama and I. S. Sogami, Langmuir **3**, 851 (1987).
[20] P. A. Hiltner and I. M. Krieger, J. Phys. Chem. **73**, 2386 (1969).
[21] R. K. Iler, *The Chemistry of Silica* (Wiley, New York, 1979), p. 19.
[22] D. O. Riese, W. L. Vos, G. H. Wegdam, F. J. Poelwijk, D. L. Abernathy, and G. Grübel, Phys. Rev. E **61**, 1676 (2000).
[23] R. S. Crandall and R. Williams, Science **198**, 293 (1977).
[24] S. Yerazunis, S. W. Cornel, and B. Winter, Nature (London) **207**, 835 (1965).
[25] J. P. Hoogenboom, D. Derks, P. Vergeer, and A. van Blaaderen, J. Chem. Phys. **117**, 11320 (2002).